

1 **Title**

2 A simple model for predicting agronomy floods in rice fields in Bicol, Philippines

3

4 **Authors**

5 Xiaojing Wei¹, Jane Girly Balanza¹, Jeny Raviz², Rowena Castilla², Airene Baradas², Alice
6 Laborte²

7

8 ¹ Alliance of Bioversity International and CIAT

9 ² International Rice Research Institute

10

11 *The paper is a non-peer reviewed preprint submitted to EarthArXiv.*

12 **Abstract**

13 Climate change is expected to intensify the impacts of flood events on agricultural production,
14 particularly in flood-prone regions like the Philippines, where rice farming is heavily affected by
15 frequent typhoons. Flood forecasting and early warning systems can aid in mitigating these
16 risks; however, the insufficient coverage of hydrometric monitoring stations and limited
17 computational resources can be barriers for developing countries. Remote sensing technology
18 offers a promising solution to bridge these gaps, providing critical hydrometric data and enabling
19 more accessible flood prediction models. Leveraging high-spatial resolution, remote sensing-
20 based flood extent data specifically developed for rice fields, we explore the possibility of
21 predicting agronomical flood extent in the Bicol region of the Philippines using a series of simple
22 logistic regression models with different lookback windows. The model predictors only included
23 rainfall at two spatial scales and flow accumulation. The best-performed model, with three-day
24 lookback window, captured 65% of variation in flooding among events. However, the best model
25 did not predict well the variation in flooding within basins, nor did it account for the heterogeneity
26 in the response of flooding to rainfall among basins. We suggested several avenues for
27 improving the model, including incorporating basin characteristics and additional predictors for
28 better capture variation in flooding within and among basins.

29

30 **Introduction**

31 Climate change is expected to exacerbate the damage caused by flood events to agricultural
32 production (Shrestha et al., 2019, Nat. Hazards). Flood forecasting and early warning services
33 have the potential to help farmers better manage these risks. In developing countries, a key
34 barrier to building and strengthening such systems is the lack of sufficient coverage of
35 hydrometric monitoring stations, which leads to a lack of historical and real-time hydrometric
36 data (Nevo et al., 2022, HESS). Besides the hydrometric data gap, the lack of sufficient
37 computation resources and technical human capacity can also prevent developing countries
38 from taking advantage of the state-of-the-art forecasting models (Shrestha, et al. 2015, Int. J.
39 Water Resour. Dev.).

40 Recent decade has seen remote sensing emerged as a promising avenue to address the
41 above-mentioned data, computation resource, and human capacity gaps. Remote sensing has
42 been employed to measure various key hydrological variables, such as river water level,
43 discharge, flood extent, topography, and soil moisture (Teng et al., 2017, Environ. Model. Softw.;
44 Ekeu-wei et al., 2018, Hydrol).

45 The potential of remote sensing addressing the above-mentioned critical gaps can be further
46 amplified by innovative modelling approaches. Flood prediction models usually include two
47 components, a rainfall-runoff model that predicts flow rate as driven by precipitation and an
48 inundation model that predicts flood extent based on flow rate. Statistical models (and more
49 recently, machine learning and deep learning models) have been used to predict the parameters
50 of rainfall-runoff models and the signature hydrologic behaviors of ungauged basins (Beven
51 2012; Nearing et al. 2020, Water Res. Manag.; Dasgupta et al. 2024, Hydro.Res). Increasingly,
52 the predictors of such models (e.g., basic characteristics) can be measured through remote

53 sensing. Similarly, to avoid the high computation cost and demanding data requirement of
54 traditional, mechanistic inundation models, a new generation of low-complexity, conceptual
55 models has been developed based on digital elevation model (hereafter DEM; Afshari, et al.
56 2018, J. Hydrol.) or remote sensing-based historical flood extent data (Chen et al. 2019,
57 Remote Sens.).

58 The Philippines experiences approximately 20 typhoons per year, each of which costs about 42
59 million USD in damage to rice production. However, flood forecasting and early warning
60 services specifically tailored to rice farmers, integrated in a climate information service (CIS)
61 system, are still unavailable to most of the Philippine rice farmers. A CIS system combines
62 information of the specific cropping system and farming practice with flood forecasting and early
63 warnings to provide actionable agricultural advisories (e.g., harvest earlier to avoid floods). Two
64 factors have likely contributed to this gap. First, like in many developing countries, in the
65 Philippines, only major river basins are gauged. Second, while flood forecasting and early
66 warning services for water level in major river basins are provided by government agencies,
67 early warning service tailored to predicting flood extent in rice fields is still lacking.

68 Here, leveraging remote sensing-based historical flood extent data product specifically
69 developed for Philippine rice fields, we explore the possibility of predicting agronomical flood
70 extent in the Bicol region of the Philippines using a series of simple logistic regression models
71 based on rainfall and digital elevation model (DEM)-derived hydrological variables.

72

73 **Method**

74 All analyses were conducted in R (R Core Team, 2024). All spatial data was manipulated using
75 the *terra* package (Hijmans, 2024).

76 Data

77 Historical flood extent data has been developed based on sentinel 2 satellite imagery (Raviz et
78 al., manuscript in preparation). These flood extent data indicate whether rice planting area in the
79 Bicol Region were submerged or not (coded as 1/0) during eight flood events (due to either
80 typhoon or tropical cyclone) from 2014 to 2019 (Table 1) at a spatial resolution of 20 m. The
81 data was resampled to 30 m to match the spatial resolution of model predictors.

82 Based on SRTM DEM data at a spatial resolution of 30 m, we delineated the boundaries of
83 watershed (watershed here is defined as an area with a single pour point into either the ocean
84 or a lake) covering all rice production area in the Bicol Region using the *whitebox* package in R
85 (Wu et al., 2022). Also using the *whitebox* package and the same DEM data, we calculated log-
86 transformed flow accumulation.

87 We obtained historical, daily rainfall from CHIRPS (de Sousa et al. 2020, J. Open Source
88 Softw.) at a spatial resolution of 5km over the 10 days before the flood event (the earliest date
89 when the SAR imagery was captured). We calculated two sets of predictors using the rainfall
90 data. First, we resampled the rainfall data to 1 km then calculated the accumulative rainfall 1, 3,

91 5, and 10 days prior to the event *over the entire watershed*. Second, we resampled the rainfall
92 to 30m and calculated the accumulative rainfall at the 30m-grid cell level.

93 Model

94 We fitted four logistic regression models with the following model formula:

95
$$\text{Likelihood of submergence of the grid cell} \sim \ln(FA) + \text{rain}_{xd_watershed} + \text{rain}_{xd_cell}$$

96 Where $\ln(FA)$ is the log-transformed flow accumulation of the cell, $\text{rain}_{xd_watershed}$ and
97 rain_{xd_cell} are rainfall over x days prior to the flood event at the watershed and the grid cell
98 level, respectively, x = 1, 3, 5, and 10 days.

99 To avoid collinearity, we fitted a linear regression model of the rain at the grid cell level against
100 the rain in the entire basin and used the residual of the former as the predictor. All predictors
101 were scaled and centered. We split the entire dataset (20,418,616 records) into 80% training
102 data and 20% testing data. We fitted the models using the *fastglm* package (Huling, 2022). We
103 determined the cutoff point by maximizing the F1 score of the training dataset using the
104 *cutpointr* package (Thiele et al. 2021, J. Stat. Softw.). We then compared the models based on
105 the F1 score of the testing dataset calculated using the optimized cutoff point.

106

107 **Results and Discussion**

108 Table 2 showed the recall, precision, F1 score, and AIC of the four models with different
109 lookback windows calculated using the test datasets. The model with a three-day window
110 showed the highest F1 score (0.27, vs. 0.26, 0.19, 0.19) and lowest AIC. Judging by the F1
111 score, overall, the model performance was low even for the best model. In all four models, the
112 likelihood of flooding significantly increased with flow accumulation, total rainfall in the basin and
113 at the grid cell level (see Table 3 for the results of the best model). Together, these results
114 suggested that the predictors that were currently included in the model were predictive of the
115 likelihood of flooding; however, substantial variation was still not captured even by the best
116 model. Below, we examined the extent to which the best model (i.e., with three-day look back
117 window) captured the observed variations in flooding among flood events, among event-basin
118 combinations, and within basins.

119 The observed percent of flooding in all rice production area in the Bicol region during a given
120 flooding event increased with the total rainfall over the period of three days before the start date
121 of the event (Pearson's correlation coefficient, hereafter $r = 0.78$, $P = 0.02$; Fig. 1a).
122 Furthermore, the mean predicted probability of being flooded increased with the observed
123 percent of flooding in all rice production area in Bicol ($r = 0.81$, $P = 0.02$; Fig. 1b). Together,
124 these results indicate that the best model captured a substantial portion of the observed
125 variation in flooding among events.

126 The observed percent of flooding in the rice production area of a given basin, during a flood
127 event did not show any significant relationship with the amount of rainfall in the basin during the
128 period of three days before the start date of the event, when examined across all basin-event
129 combinations (Fig. 2a). When examined within each single basin across the eight flood events,

130 however, the correlation between the observed percent of flooding and the amount of rainfall in
131 the basin three days before the start date of the event varied from -0.42 to 0.96 (Fig. 2b). Basins
132 that experienced a wider range of rainfall across the eight events, (which tended to be larger
133 basins), showed a more positive correlation between the observed percent of rainfall and the
134 amount of rainfall three days before the event (Fig. 2c). Together, these results suggested that
135 the basins in the Bicol region differed in their hydrological behaviors, i.e., given the same
136 amount of rainfall during the same time frame, they did not show the same percent of area
137 flooded. Due to such heterogeneity, even the best model failed to capture the variation in
138 flooding at the spatial-temporal scale among basin-event combinations (Fig. 2d).

139 Finally, to examine if the best model captured the variation in flooding within basin-event
140 combinations, we used the Bicol River Basin (BRB), the largest basin in the Bicol region, as an
141 example for the subsequent analysis. Within BRB, the amount of rainfall three days before the
142 flood event was significantly higher in flooded than not-flooded cells (Fig. 3b). This result,
143 combined with the fact that the two rainfall predictors showed similar magnitude of the
144 coefficient estimate and the statistical significance (Table 3), suggested that rainfall at both the
145 basin level and at the grid cell level influenced the likelihood of flooding at the grid cell level. In
146 contrast, despite showing a positive, significant, albeit weaker effect on the likelihood of flooding
147 in the models (Table 3), log-transformed flow accumulation did not show any significant
148 correlation with the number of times that the grid cell was flooded during the eight flood events
149 within BRB (Fig. 3c). In line with this result, the spatial variation in flow accumulation was rather
150 fine (Fig. 4c), while the observed number of times of flooding showed clustering at a coarser
151 scale (Fig. 4a), which also did not fully resemble the pattern of spatial variation of rainfall (Fig.
152 4d).

153 In summary, the best model, which has a three-day look back window, explained the observed
154 variation in flooding among events relatively well, but was not able to capture the observed
155 variation in flooding at finer spatial scales for possibly two reasons. First, our models did not
156 capture the heterogeneity in hydrological behavior among basins. Receiving the same amount
157 of rainfall (at a per area basis), basins could show differential flooding extent due to differences
158 in topography (e.g., flatter basins should be more extensively flooded, albeit with shallower
159 water depth, than basins with steeper slopes), as well as soil texture and vegetation cover.
160 Second, as illustrated by the case of BRB, our models did not fully capture the coarser pattern
161 of spatial variation in flooding within basins.

162 Based on the analyses above, our models could be improved by the following means. First, the
163 heterogeneity in the hydrologic response of the basins should be better accounted for. Existing
164 literature in regionalization has identified characteristics of basins that could be indicative of
165 their hydrologic behavior, such as slope, soil texture, and vegetation cover. A particularly
166 interesting approach to incorporate these variables in the models is using machine learning or
167 deep learning algorithms, which can better handle the non-linear effects of these additional
168 variables, including their interactions with rainfall. Furthermore, we applied the same lookback
169 windows to all basins, which significantly varied in size. A potential future direction is to explore
170 whether using shorter lookback windows in smaller basins could improve model performance.
171 Second, additional predictors should be included to better capture the coarser spatial variation

172 in flooding within basins. Such predictors could be other hydrological variables based on DEM,
173 such as height above nearest drainage and distance to major river. Notably, in rice production
174 systems, irrigation infrastructure and schedule might also influence the spatial variation of flood
175 extent. Third, we used reconstructed rainfall data to fit the models, which might not accurately
176 reflect the spatial variation of the actual rainfall and hence should be calibrated with ground
177 measurement if such data is available.

178

179 **Acknowledgement**

180 We thank A. Urfels for insightful discussion that has substantially improved the work. This study
181 was funded by the CGIAR initiative ClimBer.

182

183 **References**

- 184 Shrestha, Badri Bhakta, et al. "Assessing flood disaster impacts in agriculture under climate change
185 in the river basins of Southeast Asia." *Natural Hazards* 97 (2019): 157-192.
- 186 Nevo, Sella, et al. "Flood forecasting with machine learning models in an operational
187 framework." *Hydrology and Earth System Sciences* 26.15 (2022): 4013-4032.
- 188 Shrestha, Mandira Singh, Wolfgang E. Grabs, and Vijay R. Khadgi. "Establishment of a regional flood
189 information system in the Hindu Kush Himalayas: challenges and opportunities." *International
190 Journal of Water Resources Development* 31.2 (2015): 238-252.
- 191 Teng, Jin, et al. "Flood inundation modelling: A review of methods, recent advances and uncertainty
192 analysis." *Environmental modelling & software* 90 (2017): 201-216.
- 193 Ekeu-wei, Iguniwari Thomas, and George Alan Blackburn. "Applications of open-access remotely
194 sensed data for flood modelling and mapping in developing regions." *Hydrology* 5.3 (2018): 39.
- 195 Beven, Keith J. *Rainfall-runoff modelling: the primer*. John Wiley & Sons, 2012.
- 196 Nearing, Grey S., et al. "What role does hydrological science play in the age of machine
197 learning?." *Water Resources Research* 57.3 (2021): e2020WR028091.
- 198 Dasgupta, Rijurekha, et al. "Revisit hydrological modeling in ungauged catchments comparing
199 regionalization, satellite observations, and machine learning approaches." *HydroResearch* 7 (2024):
200 15-31.
- 201 Afshari, Shahab, et al. "Comparison of new generation low-complexity flood inundation mapping
202 tools with a hydrodynamic model." *Journal of Hydrology* 556 (2018): 539-556.
- 203 Chen, Zeqiang, et al. "RFim: a real-time inundation extent model for large floodplains based on
204 remote sensing big data and water level observations." *Remote Sensing* 11.13 (2019): 1585.
- 205 R Core Team (2024). "R: A Language and Environment for Statistical Computing". R Foundation for
206 Statistical Computing, Vienna, Austria.
- 207 Hijmans R (2024). "terra: Spatial Data Analysis". R package version 1.7-78,
- 208 Wu, Q., Brown, A. (2022). "whitebox: 'WhiteboxTools' R Frontend ". R Package version 2.2.0.
- 209 de Sousa, Kauê, et al. "chirps: API Client for the CHIRPS Precipitation Data in R." *Journal of Open
210 Source Software* 5.51 (2020): 2419.
- 211 Huling J (2022). " fastglm: Fast and Stable Fitting of Generalized Linear Models using 'RcppEigen'".
- 212 Thiele, Christian, and Gerrit Hirschfeld. "cutpointr: improved estimation and validation of optimal
213 cutpoints in R." *arXiv preprint arXiv:2002.09209* (2020).
- 214

215 **Table 1. Dates of flood events.** SAR is the abbreviation for Synthetic Aperture Radar.

Year	Event	Date of events	Date of SAR data used during the event	Earliest date of SAR data used during the event
2014	Glenda	Jul 13 - 17	Jul 16 -18	Jul 16
2016	Karen	Oct 13 - 16	Oct 15	Oct 15
2016	Nina	Dec 23 - 26	Dec 26	Dec 26
2017	Urduja	Dec 17 - 23	Dec 17 - 18	Dec 17
2018	Usman	Dec 25 -31	Dec 31	Dec 31
2019	Amang	Jan 19 - 21	Jan 21	Jan 21
2019	Ramon	Nov 12 - 20	Nov 17	Nov 17
2019	Ursula	Dec 24 -26	Dec 25	Dec 25

216

217

218 **Table 2. Recall, precision, F1 scores, and AIC of the four models of different lookback windows**
 219 **calculated using the test datasets.**

Look back window (d)	Recall	Precision	F1 score	AIC
1	0.23	0.16	0.19	8184816
3	0.48	0.18	0.27	7858276
5	0.48	0.18	0.26	7926545
10	0.23	0.16	0.19	8127115

220

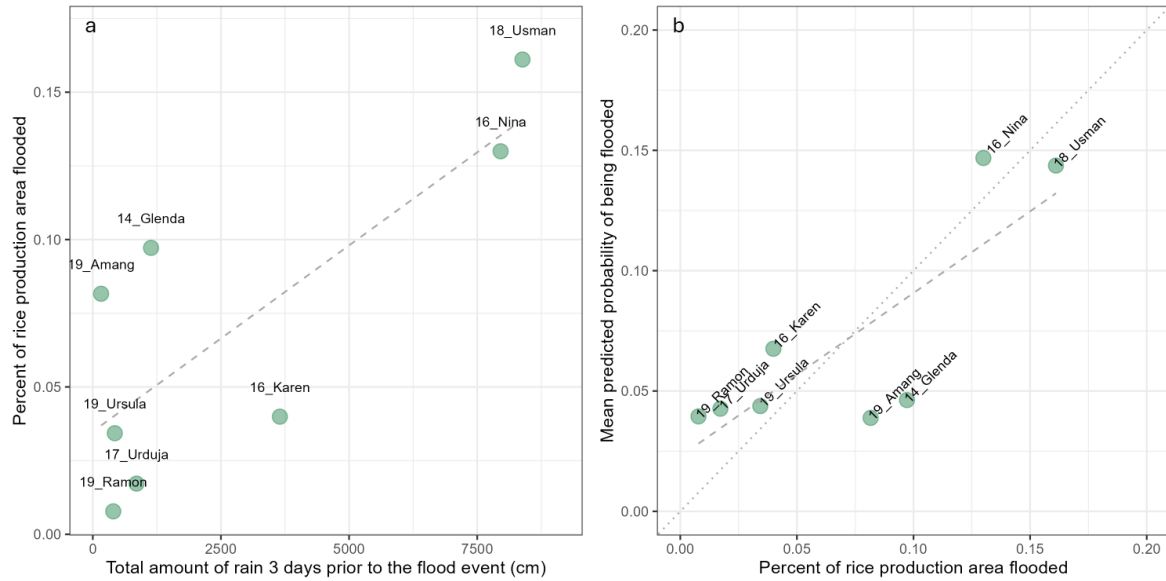
221

222 **Table 3. Coefficient estimate of predictors of the best model (with a three-day lookback window).**

223 All predictors are scaled and centered and showed a significant effect ($P < 0.001$).

Term	Coefficient estimate
Log-transformed flow accumulation	0.106
Rainfall three days before event in the basin	0.451
Residual of rainfall three days before event in the cell	0.400

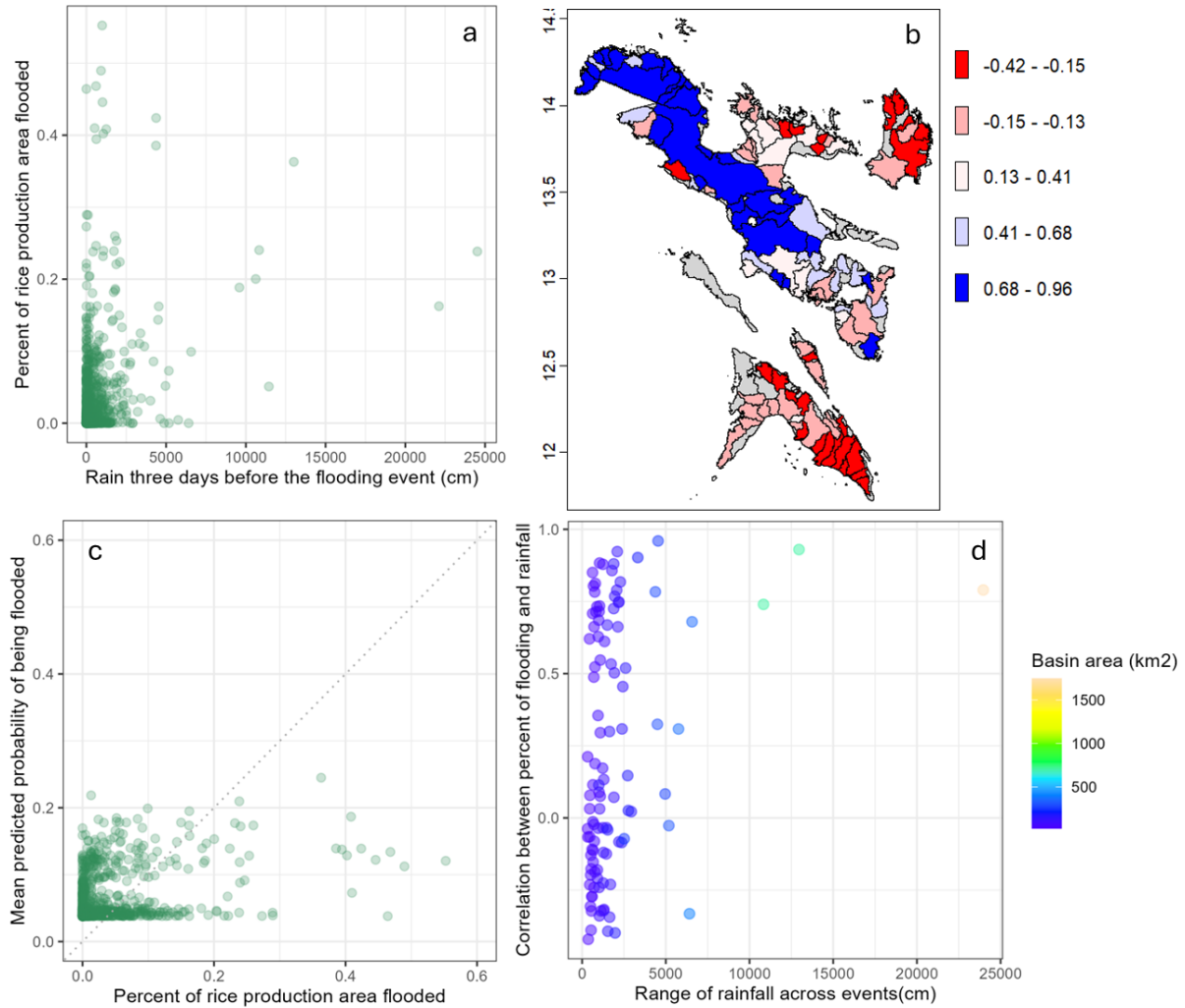
224



225

226 **Fig. 1 Variation in rainfall, as well as observed and predicted flooding among events.** a) The
 227 observed percent of rice production area flooded during a given flood event increased with the total
 228 rainfall over the period of three days before the start date of the flood event (Pearson's correlation
 229 coefficient $r = 0.78$, $P = 0.02$). b) The observed percent of rice production area flooded during a given
 230 flood event was positively correlated with mean predicted probability of being flooded in the rice
 231 production area in the Bicol region ($r = 0.81$, $P = 0.02$). Each green dot represents data pertains to a flood
 232 event. The dashed lines are the least square regression lines. The dotted line is the 1:1 line.

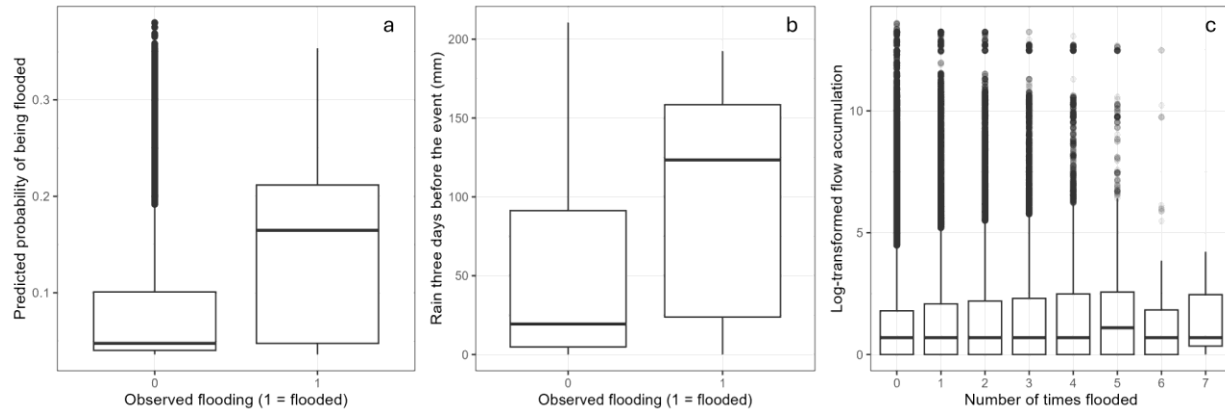
233



234

235 **Fig. 2 Variation in rainfall, as well as observed and predicted flooding among basin-event**
 236 **combinations.** When examined across all basin-event combinations, the percents of rice production area
 237 flooded in a basin did not show any significant correlation with the amount of rainfall within the basin over
 238 the period of three days before the start of the flooding event. Each green dot indicates data pertaining to
 239 a basin-event combination. b) A map of Pearson's correlation coefficient between the percents of rice
 240 production area flooded in a basin during an event versus the amount of rainfall during the period of three
 241 days before the start of flooding event, calculated for each basin individually. Blue and red hue indicate
 242 positive and negative correlation, respectively. The area colored in grey did not have rice production area.
 243 c) Mean predicted probability of flooding in a basin during an event showed a positive, significant, albeit
 244 weak correlation with the observed percents of rice production flooded in the basin during the event ($r =$
 245 0.33 , $P < 0.001$). Each green dot indicates data pertaining to a basin-event combination. The dotted line is
 246 the 1:1 line. d) Basins that experienced a wider range of rainfall across the eight events, which tended to
 247 be larger basins, tended to show a more positive correlation across the eight events between the
 248 percents of rice production area flooded versus the amount of rainfall in the basin over the period of the
 249 three days before the start of the event. Each point indicates data pertaining to a basin.

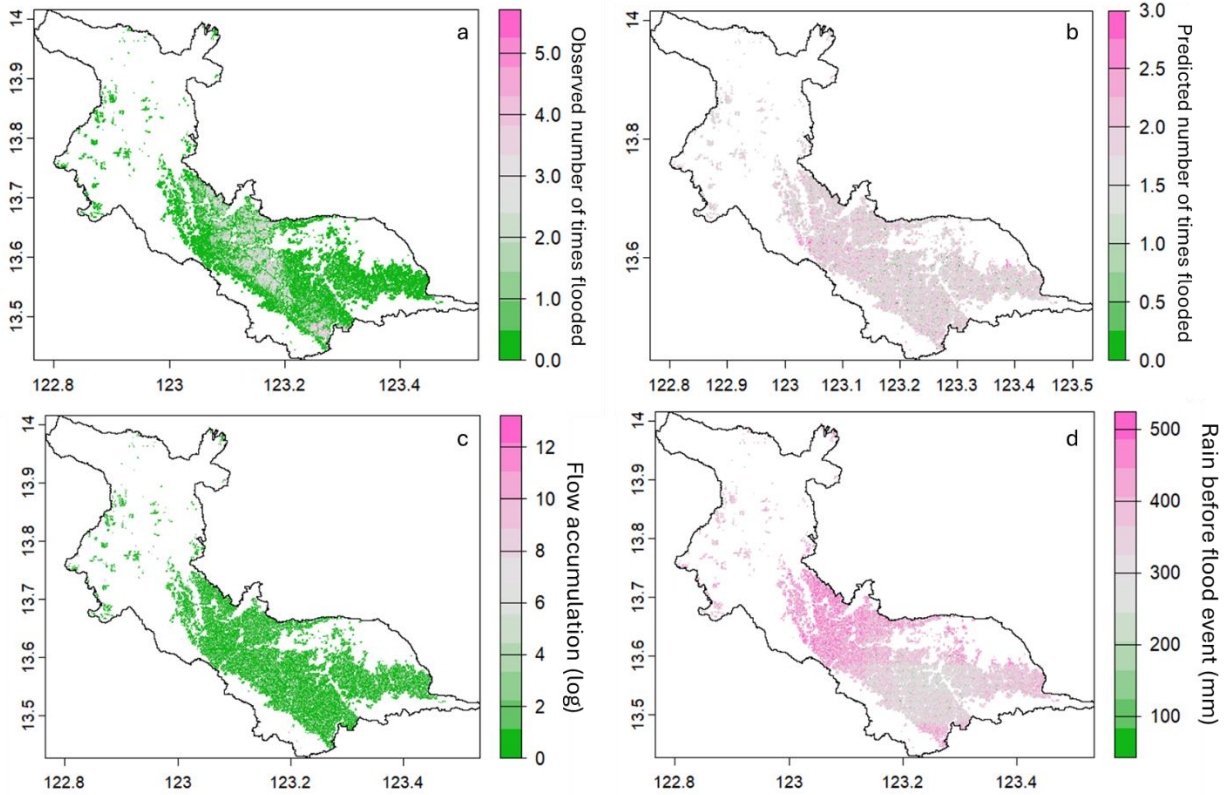
250



251

252 **Fig. 3 Effects of rainfall and flow accumulation on flooding at the grid cell level in Bicol River**
 253 **Basin.** a) The mean probability of a cell being flooded during a flood event, as predicted by the best
 254 model, was higher in cells that were flooded than in non-flooded cells. b) The amount of rainfall fell within
 255 the grid cell three days before the start of the flood event was significantly higher in cells that were
 256 flooded than in non-flooded cells. c) No significant correlation between log-transformed flow accumulation
 257 versus the number of times a cell being flooded within BRB ($r = 0.05$).

258



259

260 **Fig. 4 Spatial patterns of the observed and predicted flooding, flow accumulation and rainfall**
 261 **before the flood events.** a) and b) The observed and predicted number of times that a grid cell
 262 flooded during the eight flood events, respectively. c) Log-transformed flow accumulation. d). The mean
 263 rainfall three days before the start of the flood event averaged across the eight flood events.